

Cloning, Overexpression, and Purification of Aminoglycoside Antibiotic 3-Acetyltransferase-IIIb: Conformational Studies with Bound Substrates[†]

Michael A. Owston and Engin H. Serpersu*

The Center of Excellence for Structural Biology and the Department of Biochemistry and Cell and Molecular Biology,
The University of Tennessee, Walters Life Sciences building, M407 Knoxville, Tennessee 37996-0840

Received May 14, 2002; Revised Manuscript Received July 11, 2002

ABSTRACT: Aminoglycoside 3-acetyltransferase-IIIb (AAC3), which acetylates N₃ amine of aminoglycoside antibiotics, was cloned from *P. Aeruginosa* and purified from overexpressing *E. coli* BL21 (DE3) cells. Bound conformations of kanamycin A and ribostamycin, in the active site of the enzyme that modifies the essential N_{3B} of aminoglycoside antibiotics, were determined by NMR spectroscopy. Experimentally determined interproton distances were used in a simulated annealing protocol to determine enzyme-bound conformations of both antibiotics. Two conformations, consistent with the NOE restraints, were determined for ribostamycin. The only difference between the two conformers was the orientation of the A ring with respect to the rest of the molecule. The average glycosidic dihedral angles were $\Phi_{1A} = -22^\circ \pm 3$ and $\Psi_{1A} = -42^\circ \pm 1$ (conformer 1) and $\Phi_{1A} = -67^\circ \pm 0.7$ and $\Phi_{1A} = -59^\circ \pm 0.8$ (conformer 2). Three conformers were determined for the enzyme-bound kanamycin A. Two conformers of kanamycin A were matched well with the two conformers of ribostamycin when the A and the B rings of the antibiotics were superimposed. Conformations of kanamycin A and ribostamycin were compared to those of other aminoglycosides that are bound to different enzymes and RNA. The results lend further support to our earlier hypothesis that the A and B rings of aminoglycosides adopt a conformation that is recognized not only by the aminoglycoside-modifying enzymes but also by RNA (Serpersu, E. H., Cox, J. R., Digiammarino, E. L., Mohler, M. L., Akal, A., Ekman, D. R., and Owston, M. (2000) *Cell Biochem. Biophys.* 33, 309–321). These results may be useful in designing new antibiotics to combat the antibiotic resistance against infectious diseases.

Aminoglycoside antibiotics are broad-spectrum antibiotics used for treating various bacterial infections. They were among the earliest antibiotics to reach clinical usage (1). Aminoglycoside antibiotics bind to the bacterial 30 S ribosomal subunit, specifically to 16s RNA, and interfere with the normal protein biosynthesis, which eventually leads to cell death (2,3). They are used for the treatment of serious infections caused mostly by *staphylococci* and *enterococci*. The clinical effectiveness of these antibiotics is significantly reduced by the emergence of strains resistant to their action. The covalent modification of aminoglycoside antibiotics, by enzymes expressed in pathogenic bacteria, leads to their detoxification (4, 5). Today, there are more than 50 aminoglycoside antibiotic-modifying enzymes known to be expressed in pathogenic bacteria (6).

One of the largest groups of aminoglycoside antibiotics is where the aglycone is 2-deoxystreptamine (2-DOS). Generally, these aminoglycosides are 4,5- or 4,6-substituted at the DOS ring and can be pseudotri-, tetra-, or pentasaccharides (Figure 1). The substituents on the DOS ring are numbered 1–6, and this ring is labeled as the unprimed ring or ring B. Aminoglycosides with a 4,5- or 4,6-substituted DOS ring can also be classified as neomycin- and kanamycin-type antibiotics, respectively. The sugar ring, attached

by a glycosidic linkage to the 4-position of the DOS ring, is labeled as the prime (') ring or ring A. The sugar ring, attached by a glycosidic linkage to the 5- or 6-position of the DOS ring, is labeled as the double prime (") ring or ring C.

Aminoglycoside-modifying enzymes are promiscuous with respect to the aminoglycoside substrates, and the same enzyme can modify several structurally different aminoglycoside antibiotics (4–6). Furthermore, any given antibiotic can be modified by many different enzymes at the same or different site(s) on the antibiotic. Thus, aminoglycoside–enzyme interactions not only provide excellent opportunity to study ligand–enzyme interactions, but these studies may also provide useful leads for drug design to combat antibiotic resistance. Our laboratory is involved in the determination of enzyme-bound conformations of aminoglycosides in the active sites of different aminoglycoside-modifying enzymes using NMR spectroscopy (7–13). These studies revealed conformational similarities between different antibiotics that are bound to the same or different enzymes. Crystal structures of several aminoglycoside-modifying enzymes were determined by X-ray crystallography (14–18). However, these studies did not reveal a detailed conformation of any enzyme-bound aminoglycoside antibiotic. Only recently was the crystal structure of the aminoglycoside–3'-phosphotransferase-IIIa (APH3') solved with bound kanamycin A and neomycin B (19).

[†] This work was supported by a grant from NSF (MCB 01110741) and the Petroleum Research Fund (PRF# 32874-AC4).

* Corresponding author. Tel.: (865) 974-2668. Fax: (865) 974-6306. E-mail: serpersu@utk.edu.

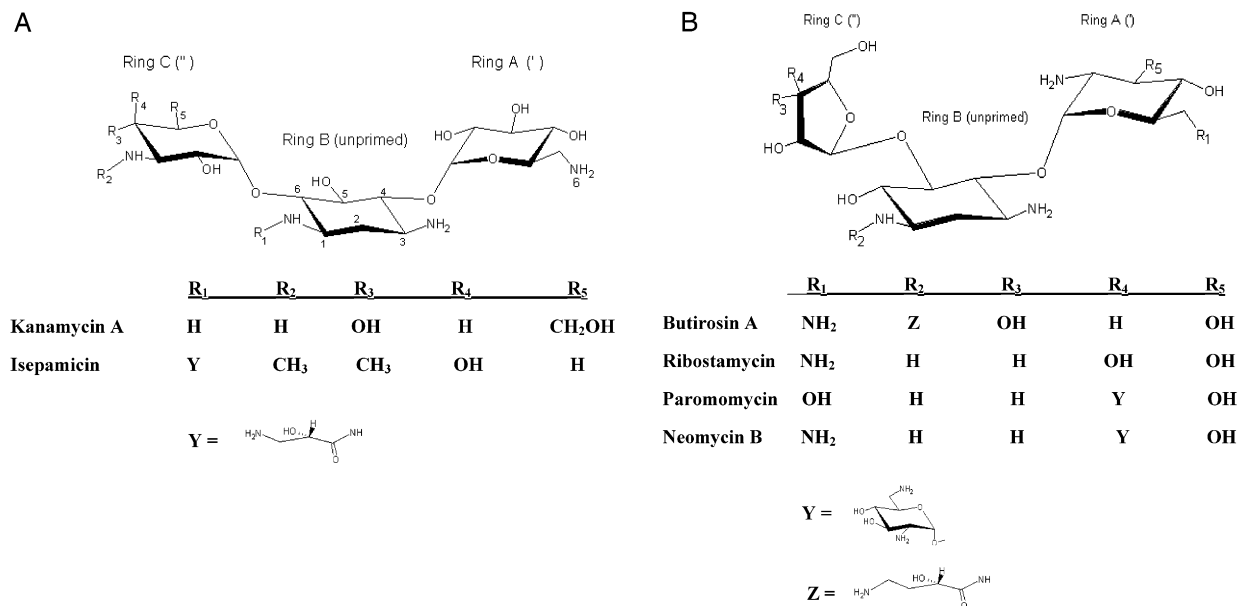


FIGURE 1: Substituents on the DOS ring are numbered 1–6, and this ring is labeled as the unprimed ring or ring B. The sugar ring, attached by a glycosidic linkage to the 4-position of the DOS ring, is labeled as the prime (') ring or ring A. The sugar ring, attached by a glycosidic linkage to the 5- or 6-position of the DOS ring, is labeled as the double prime (") ring or ring C.

Conformations of enzyme- and RNA-bound aminoglycosides were determined by NMR spectroscopy (20–22). On the basis of these NMR studies, we suggested that there might be a common structural motif that is recognized not only by the aminoglycoside-modifying enzymes but also by RNA (11–13). However, to date, data from an enzyme that can modify the central 2-deoxystreptamine (2-DOS) ring have not been available. Therefore, this work was undertaken to determine conformations of aminoglycoside antibiotics in the active site of the aminoglycoside–3-acetyltransferase-IIIb (AAC3), which acetylates the essential 3-NH₂ of the 2-DOS Ring. This manuscript describes enzyme-bound conformations of kanamycin A and ribostamycin and their comparison to earlier work, and the results support our earlier findings that the A and the B rings of aminoglycosides adopt a very similar conformation in the active site of different enzymes. A preliminary account of this work was presented earlier (23).

EXPERIMENTAL PROCEDURES

Materials. Kanamycin A and ribostamycin (Figure 1) were obtained from Sigma Chemical Co. Growth media (Yeast extract, tryptone) was from Difco. The plasmid pET-22b+, Deep Vent DNA polymerase was from New England Biolaboratories. Restriction enzymes, T4 DNA ligase, and Plasmid extraction kits were purchased from Promega.

Cloning of AAC3. The R-plasmid containing the AAC3 gene was isolated from the clinical isolate of *Pseudomonas aeruginosa* using a standard kit (Promega) with no modifications in protocol. The clinical isolate of this organism was kindly provided by Drs. George Miller and Karen Shaw of Schering Plough. The AAC3 gene was amplified by PCR and was cut with restriction endonucleases (*Nde*I and *Not*I)

allowing the gene to subsequently be put in correct orientation into the plasmid pET-22b+ (which was cut with the same enzymes), and T4 DNA ligase was used to ligate the fragment into the vector. The presence and orientation of the gene was confirmed by sequence analysis. *Escherichia coli* strain BL21 (DE3) was transformed with the pET22b-AAC3 plasmid, and the bacteria containing the plasmid was selected for on media containing kanamycin A and ampicillin (25 mg/L each).

Isolation of AAC 3. The transformed cells were grown in LB media (37 °C) containing ampicillin and kanamycin A (25 mg/L each). The culture was induced with 1 mM IPTG. Cells were grown overnight and were then pelleted and washed with STE buffer (NaCl 50 mM, TrisHCl 50 mM, EDTA 5mM, pH 7.5), and then lysed using a French Press. The cell lysate was centrifuged at 28 000g, and the pellet was saved. The pellet contained AAC3 in inclusion bodies in relatively large amounts compared to other proteins as visualized on SDS–PAGE.

Inclusion bodies were homogenized and washed with 1% Triton X-100 (v/v) in 10 mL of 50 mM sodium phosphate buffer (pH 7.5) three times and then washed three times in 10 mL of 50 mM Tris-HCl (pH 7.5). A 0.1 g sample of the pellet was then solubilized in 1 mL of 8M urea solution (pH 8.0), centrifuged to remove insoluble material, and dialyzed for 4 h against 200 mL solution of 5 mM Tris buffer (pH 7.5) containing 1 mM MgCl₂ and 5 mM NaCl. After the first dialysis step, DNase and RNase were added, and the solution was incubated at room temperature for 15 min. The enzyme solution was then dialyzed three more times against the same buffer and lyophilized. The enzyme was resolubilized in small amount of 5mM sodium phosphate buffer and purity, was visualized by SDS–PAGE, which was greater than 90% based on densitometry measurements.

Assay for activity of AAC3. A protocol used to determine activity of other acetyltransferases, with modifications described below, was used to determine AAC3 activity (24, 25). The reaction mixture contained 0.75 mM 4,4'-dithio-

¹ Abbreviations: AAC3, aminoglycoside–3-acetyltransferase-IIIb; ANT2'', aminoglycoside–2''-nucleotidyltransferase-Ia; 2-DOS, 2-deoxystreptamine; AAC6'-II, aminoglycoside–6'-acetyltransferase-II; APH3'-IIIa, aminoglycoside–3'-phosphotransferase-IIIa.

dipyridine, 0.01–0.5 mM kanamycin A, 0.01–0.25 mM acetyl CoA, 25 mM TrisHCl (pH 7.5), and 0.5 mM EDTA, in a final volume of 1 mL. The reaction was started by the addition of the enzyme. The amount of CoA formation was monitored continuously by measuring the absorbance at 324 nm using an extinction coefficient of $19\,800\text{ M}^{-1}\text{cm}^{-1}$ for the product pyridine-4-thiolate. Appropriate range of substrate concentration was used to determine kinetic parameters. Specific activity of the enzyme was $5\text{ }\mu\text{mol/min/mg}$ with kanamycin A as substrate, which yielded a k_{cat} of $\sim 2\text{ s}^{-1}$. This value is well within the range observed for aminoglycoside-modifying enzymes ($0.1\text{--}100\text{ s}^{-1}$). Kinetic studies also yielded K_{M} values of 14 ± 2.8 and $26 \pm 3.5\text{ }\mu\text{M}$ for Kanamycin A and Ribostamycin, respectively. These values are similar to K_{M} values observed for these antibiotics with other aminoglycoside-modifying enzymes.

Product Verification. A small amount of AAC3 was added to a solution containing 2 mM acetyl-CoA and 2 mM kanamycin A in 50 mM sodium phosphate buffer and 5 mM MgCl_2 . The reaction was allowed to proceed to completion, which was followed by NMR spectroscopy. Several 1D and 2D NMR spectra were acquired to verify that the kanamycin A was modified at the correct position. A very large downfield shift of the hydrogen at position 3 on the center ring from 3.06 to 3.8 ppm, consistent with the presence of a carbonyl group at the N_3 , was observed. TOCSY experiments confirmed the assignment of this resonance to be $\text{H}_{3\text{B}}$, thus confirming that the product is acetylated at the $\text{N}_{3\text{B}}$. Other chemical shift changes expected as a result of this reaction were also observed. Any other product that might be present would represent less than 5% of the main product under these conditions.

NMR Spectroscopy. Protonated solutes in the enzyme solution as well as water were replaced by deuterated counterparts using a series of dilutions and concentrations in an ultrafiltration unit. Coenzyme A and the aminoglycoside substrate were titrated into an NMR tube that contained 250 μM AAC3 in 5 mM phosphate buffer pH 7.5. Coenzyme A instead of acetyl-CoA was used to prevent acetylation of the antibiotics. The final concentrations of CoA and aminoglycoside were equal to one another and in 10 times excess of the protein. Kanamycin A and ribostamycin were used as substrates in separate experiments. A series of 2D TRNOESY experiments were performed using 30, 60, 90, and 120 ms mixing times. NOE build-up curves were linear for the mixing times used, and NOE intensities were determined from the spectra obtained with 90 ms mixing time. QUIET-NOESY (26, 27) experiments were also performed by systematically inverting the different regions of the spectrum. A Gaussian Cascade Q3 pulse was used in the middle of the mixing period to invert selected regions of the spectrum in the QUIET-NOESY experiments. A total of 228–256 FIDs of 1408 complex data points were collected. The spectral width was 5479 Hz, and 80–128 scans per FID were acquired. In all NOESY spectra, the data were multiplied by a \sin^2 window function in both dimensions before Fourier transformation. Enzymatic activity was tested before and after the experiments, and no significant loss was observed during the NMR experiments.

All NMR experiments were performed on a 600 MHz Varian Inova instrument equipped with a single gradient axis

and a triple resonance probe for the observation of proton, carbon, and nitrogen nuclei.

Data Analysis and Structure Determination. NMR data was processed with Felix 2000 software operating on a Silicon Graphics Indigo 2 workstation. The data were multiplied by a sine bell-squared window function in both dimensions before Fourier transformation. The assignments of the peaks of kanamycin A and ribostamycin were from previous studies (11, 28). Cross-peak intensities observed in NOE experiments were divided into three categories as strong, medium, and weak. These intensities were converted into distance restraints based upon the comparison to the cross-peak volume of $\text{H}_{1\text{A}}$ to $\text{H}_{2\text{A}}$, which has a known distance of $2.38 \pm 0.1\text{ }\text{\AA}$. Interproton distance restraints used were as follows: strong, 2.0–2.7 \AA ; medium, 2.0–3.6 \AA ; weak, 2.0–4.5 \AA . All calculations were carried out using the AMBER force field interfaced with DISCOVER (Molecular Simulations) on the same workstation. The atom potential types and charges were set according to Homan's potential types for carbohydrates (29) in the AMBER force field. NMR derived restraints were applied to the aminoglycosides, and a series of dynamics and minimization steps were performed. Random structures were created by unrestrained molecular dynamics at 600 K. Then the NMR derived distance restraints were applied and a series of dynamics used decreasing temperatures 400, 350, 300, and 200 K for 500 ps, each followed by a minimization (until $\text{RMSD} < 0.01\text{ kcal/\AA}$), were used in a simulated annealing protocol. The final structures were then subjected to unrestrained molecular dynamics simulation at 300 K to eliminate virtual conformations. The force constant for the distance restraints was $50\text{ kcal/mol }\text{\AA}^{-2}$. The dielectric constant used in the above experiments was 4.0. Using this simulated annealing protocol, a set of 20 or more structures that are consistent with the NOE restraints were obtained and analyzed to determine the AAC3-bound structures of the aminoglycosides kanamycin A and ribostamycin (Table 1).

RESULTS AND DISCUSSION

We initially attempted to use the antibiotic isepamicin in our studies since the conformation of this antibiotic was already determined in several enzyme-antibiotic complexes (10, 11, 13). However, observation of only a limited number of NOEs and the weakness of them precluded a meaningful structure determination with this antibiotic in the AAC3–CoASH–Isepamicin complex. This is not surprising since the K_{M} of isepamicin was determined to be 0.5 mM, which is significantly higher than the K_{M} values of the other aminoglycosides. Therefore, kanamycin A and ribostamycin, which yielded acceptable NOE data, were used instead.

Conformation of Ribostamycin in the active site of AAC3. A total of 22 structures, consistent with the NOE restraints, were determined for the enzyme-bound ribostamycin. Even a visual inspection of the structures (Figure 2) clearly shows that these structures are divided into two major conformers (conformer 1 and conformer 2). Data analysis using the glycosidic angles $\Phi_{1\text{A}}$ ($\text{H}_{1'}\text{--C}_{1'}\text{--O}\alpha\text{--C}_4$), $\Phi_{1\text{A}}$ ($\text{H}_4\text{--C}_4\text{--O}\alpha\text{--C}_{1'}$), $\Phi_{1\text{C}}$ ($\text{H}_{1''}\text{--C}_{1''}\text{--O}\beta\text{--C}_5$), and $\Phi_{1\text{C}}$ ($\text{H}_5\text{--C}_5\text{--O}\beta\text{--C}_{1''}$) shows a much better fit (i.e., significantly smaller RMSD values) if the structures are divided into two conformers as shown in Table 1. It is clear from these data

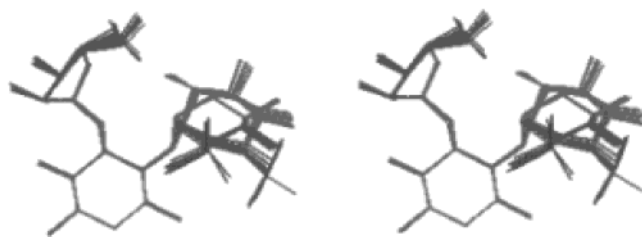


FIGURE 2: AAC3-bound ribostamycin structures as determined by restrained simulated annealing. All 22 structures are shown in stereo as superimposed at the B ring.

that the A ring of ribostamycin can have two different orientations with respect to the B ring. The average angles for conformer 1 of ribostamycin were as follows: $\Phi_{1A} = -22^\circ \pm 3$, $\Psi_{1A} = -42^\circ \pm 1$, $\Phi_{1C} = -9^\circ \pm 4$, and $\Psi_{1C} = 51^\circ \pm 1$. For conformer 2, they are as follows: $\Phi_{1A} = -67^\circ \pm 0.7$, $\Psi_{1A} = -59^\circ \pm 0.8$, $\Phi_{1C} = -9^\circ \pm 3$, and $\Psi_{1C} = 49^\circ \pm 1$. The orientation of the B and C rings was the same in both conformers, yielding an overall RMSD of 0.102 for these rings. Both conformers show no violation of NOE restraints; however, these data cannot exclude the possibility that only one of the conformers may represent the actual enzyme-bound ribostamycin and the other may be simply a conformation that satisfies the NOE restraints. An unrestrained dynamics simulation study showed that the conformers interconvert; however, such conversion may be sterically hindered in the active site of AAC3. Observation of multiple conformations may be due to the lack of large number of inter-ring NOE restraints, which is common with carbohydrate molecules. However, in an earlier study we

Table 1: Statistics of NMR Data and Structures

	kanamycin A	ribostamycin
Distance Restraints		
total restraints	38	18
inter-ring restraints	2	2
strong (2.0–2.7 Å)	10	4
medium (2.0–3.6 Å)	11	7
weak (2.0–4.5 Å)	17	7
Pairwise rmsd (Å) for the Final Structures		
rings A and B heavy atom		
all structures	0.729 ± 0.467	0.300 ± 0.285
conformer 1	0.011 ± 0.007	0.026 ± 0.011
conformer 2	0.044 ± 0.032	0.034 ± 0.020
conformer 3	0.010 ± 0.006	
Glycosidic Angles for Conformers (deg)		
ψ AB		
conformer 1	-10.8 ± 2.5	-22.1 ± 2.8
conformer 2	-8.0 ± 3.6	-67.4 ± 0.7
conformer 3	-72.5 ± 0.6	—
ψ AB		
conformer 1	-45.0 ± 3.1	-42.1 ± 1.2
conformer 2	48.0 ± 1.7	-59.0 ± 0.8
conformer 3	-56.7 ± 0.2	
ψ BC		
conformer 1	-8.88 ± 4.5	-9.4 ± 4.3
conformer 2	-17.9 ± 2.2	-9.3 ± 3.3
conformer 3	-14.0 ± 0.5	—
ψ BC		
conformer 1	49.0 ± 2.3	51.0 ± 1.4
conformer 2	-41.8 ± 1.7	48.6 ± 1.2
conformer 3	51.5 ± 0.2	—

observed two conformations for ribostamycin in the active site of the aminoglycoside-3'-phosphotransferase-IIIa, despite the presence of several inter-ring NOE restraints including a couple between the rings A and C (11).

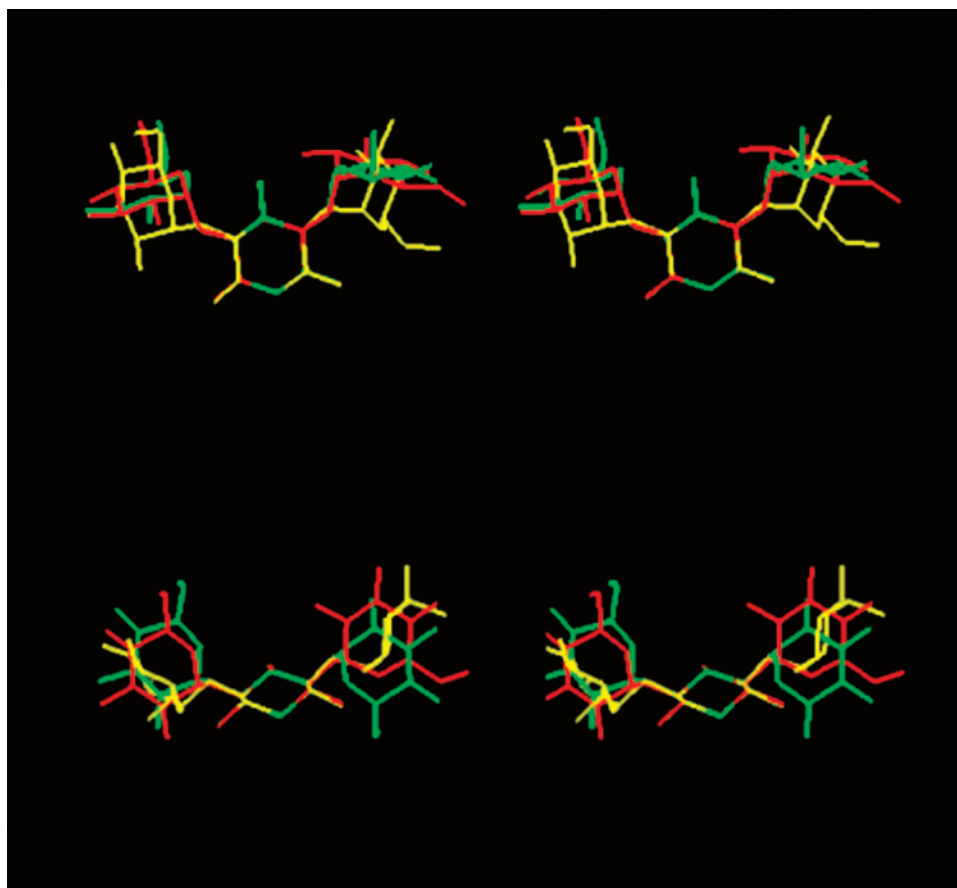


FIGURE 3: Structures determined for kanamycin A bound to AAC3. Structures are shown as stereopairs, and each conformer is represented with a single structure for simplicity: conformer 1 (red), conformer 2 (green), and conformer 3 (yellow). Two different views are shown.

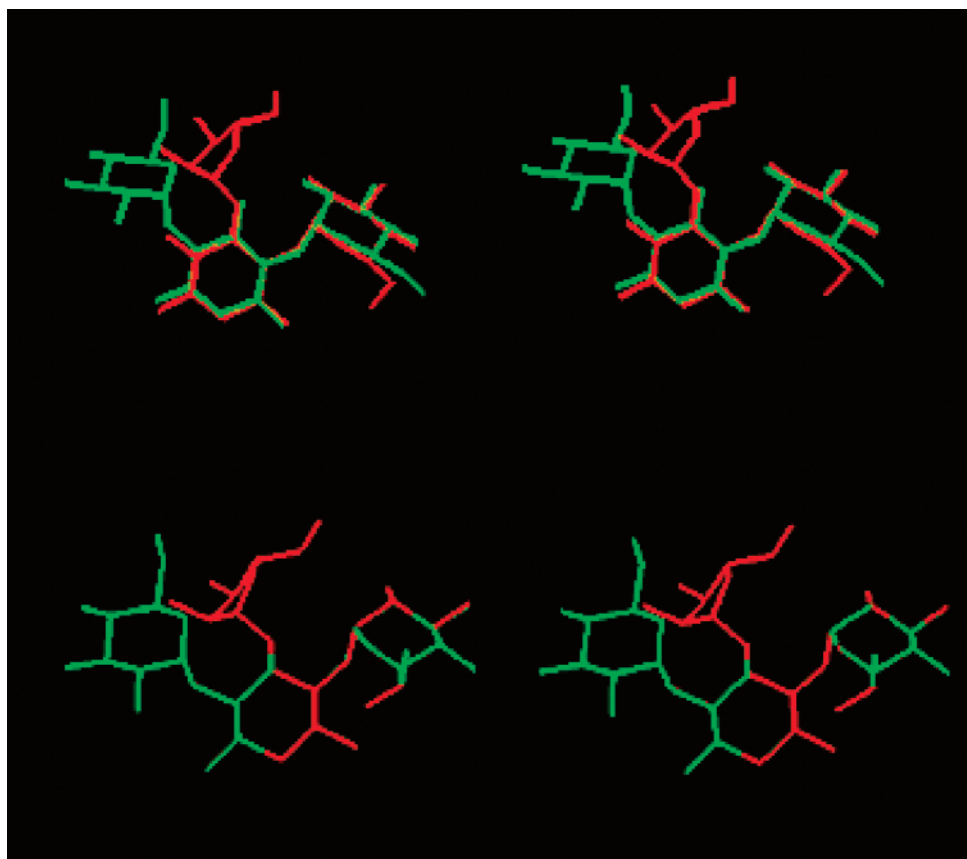


FIGURE 4: Comparison of the AAC-bound conformations of kanamycin A and ribostamycin. (top) A stereoview of the conformer 1 of ribostamycin vs the conformer 1 of kanamycin A and (bottom) stereoview of the conformer 2 of ribostamycin vs the conformer 3 of kanamycin A. The rings A and B were superimposed in both comparisons.

Conformation of Kanamycin A in the Active Site of AAC3. Kanamycin A also yielded multiple conformations that satisfied the NOE restraints. The structures were divided into three conformers based on the analysis of the glycosidic dihedral angles (Table 1). The average dihedral angles were as follows: conformer 1 (nine structures), $\Phi_{1A} = -11 \pm 3$, $\Psi_{1A} = -45 \pm 3$, $\Phi_{1C} = -9 \pm 4$, and $\Psi_{1C} = 49 \pm 2$; conformer 2 (six structures), $\Phi_{1A} = -8 \pm 3$, $\Psi_{1A} = 48 \pm 2$, $\Psi_{1C} = -18 \pm 2$, and $\Psi_{1C} = -42 \pm 2$; and conformer 3 (five structures), $\Phi_{1A} = -73 \pm 0.6$, $\Psi_{1A} = -57 \pm 0.2$, $\Phi_{1C} = -14 \pm 0.5$, and $\Psi_{1C} = 51 \pm 0.2$. Figure 3 shows an overlay of the three different conformers. None of the conformers showed any violation of the NOE restraints; however, as mentioned earlier, some of the conformations may be just consistent with the NOE restraints but may not represent the enzyme-bound kanamycin A. Inspection of the data suggests that the conformer 2 is significantly different from the others. Conformers 1 and 3 are very similar to each other with respect to the orientation of the B and C rings, and in fact, an RMSD value of 0.031 was determined when these rings are superimposed.

Comparisons between ribostamycin and kanamycin conformations. Despite the differences in their structures, the enzyme-bound kanamycin A and ribostamycin show significant conformational similarities. For example, when the conformer 1 of ribostamycin and the conformer 1 of kanamycin A were overlaid at the A and B rings, an RMSD value of 0.15 was observed. Figure 4 shows this comparison. This observation is consistent with our earlier data and lends further support to our hypothesis that the A and the B rings

represent the main conformational unit of aminoglycosides that is recognized by the aminoglycoside-modifying enzymes (12, 13). Thus, these conformers may represent the enzyme-bound conformations of both antibiotics.

Figure 4 also shows a similar comparison made between the conformer 2 of ribostamycin and the conformer 3 of kanamycin A. Again, the similarity of the structures are clearly visible, and an RMSD of 0.028 was determined for the super positioning of the A and the B rings between the two conformers. Since the conformer 3 of kanamycin A is a minor conformer, these conformations may either represent the minor enzyme-bound conformations, or they may be simply consistent with NOE restraints but does not exist in the active site of AAC3. However, one should keep in mind that the aminoglycoside-modifying enzymes are capable of accepting several structurally different aminoglycosides as substrates. This suggests that the active sites of these enzymes may show some flexibility to accommodate several substrates or multiple conformations of the same substrate. A recent crystallographic study suggests that the basis of the substrate promiscuity is the presence of alternative sites in the antibiotic binding site of the aminoglycoside-3'-phosphotransferase-IIIa (19), which is consistent with our observations. These comparisons also suggest that the conformer 2 of kanamycin A is unlikely to represent the enzyme-bound kanamycin A since it is significantly different from the other conformers of kanamycin A and ribostamycin.

Comparisons to other enzyme bound aminoglycosides. Our earlier studies, using several different aminoglycoside antibiotics and different aminoglycoside-modifying enzymes,

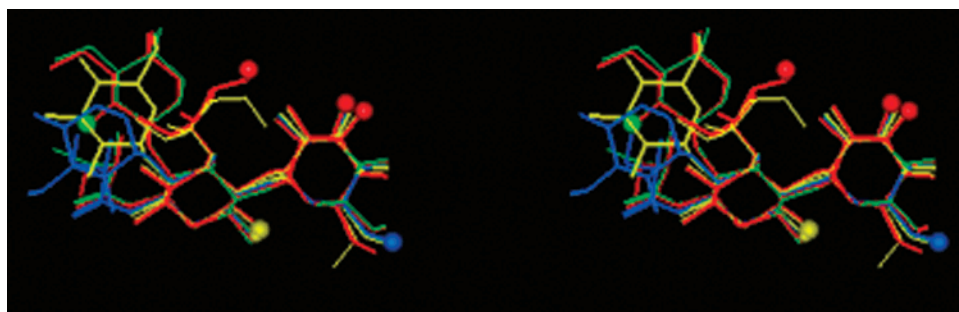


FIGURE 5: Stereoview of enzyme-bound conformations of isepamicin and ribostamycin (red, bound to APH3') (11), isepamicin (blue, bound to AAC6') (10), isepamicin (green, bound to ANT2'') (13), and kanamycin A and ribostamycin (yellow, bound to AAC3) (this work). All structures are overlaid at the A and B rings.

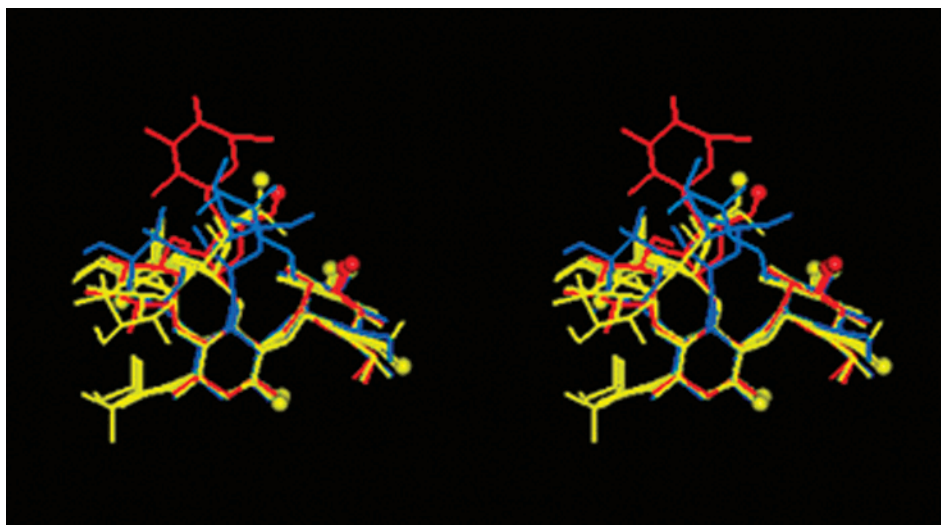


FIGURE 6: Stereoview of enzyme/RNA-bound conformations of aminoglycoside antibiotics. All enzyme-bound structures (yellow) are from Figure 7 (NMR). Blue structures are RNA-bound gentamycin (21) and paromomycin (only three rings shown for simplicity) (20) (NMR). Red structures are APH3'-bound kanamycin A and neomycin B (X-ray crystallography) (19). All structures are overlaid at the A and B rings.

which included aminoglycoside-3'-phosphotransferase-IIIa (APH3'), aminoglycoside-6'-acetyltransferase-Ib (AAC6'), and aminoglycoside-2'-nucleotidyltransferase (ANT2''), suggested that there might be a shared conformational motif among the enzyme-bound antibiotics that is recognized by different enzymes (7–13). This was based on the observation of the superimposed A and B rings of several enzyme-bound aminoglycosides. Conformers 1 of ribostamycin and kanamycin A, determined in this work, are also consistent with this idea. Figure 5 shows the superpositioned conformations of several enzyme-bound aminoglycoside antibiotics determined by NMR spectroscopy in our laboratory. These structures were overlaid at the A and B rings, and several significant points need to be emphasized in this comparison. The first point is to realize that several structurally different aminoglycosides are compared, and yet their conformation about the A and the B rings are virtually superimposable. Another important aspect of this comparison is the fact that all three types of aminoglycoside modification (an *O*-phosphotransfer, an *O*-nucleotidyltransfer, and two different *N*-acetyltransfer reactions) are also represented in this comparison. Finally, the modification of the all three major rings, including the ring C, of the aminoglycosides is also represented. As shown in Figure 5, the target atoms are located in different parts of the antibiotics; therefore, access to these sites must occur by the proper orientation of both substrates in the active site. On the basis of these observations

and the comparison shown in Figure 5, we feel that the similarity of the conformations about the A and the B rings may apply to all or most of the aminoglycoside-enzyme complexes, which may have significant implications in drug design against infectious diseases.

Comparison to RNA Bound Aminoglycosides and Crystallographic Studies. All of the conformations shown in Figure 5 were determined by NMR. Recently, the crystal structure of the aminoglycoside-3'-phosphotransferase-IIIa with bound aminoglycosides became available (19). When the enzyme-bound conformations of neomycin B and kanamycin A were superimposed with the conformations determined by NMR (Figure 6), an excellent agreement was observed with respect to the orientation of the A and the B rings, yielding RMSD values of 0.109 and 0.175 for neomycin B and kanamycin A, respectively. In addition, conformations of gentamycin C_{1a} and paromomycin that was determined by NMR in RNA-aminoglycoside complexes also showed a remarkable similarity to the enzyme-bound conformations of different aminoglycosides at the A and the B rings. Similarly, the crystal structure of paromomycin in ribozyme-paromomycin complex (30) yields an RMSD of 0.15 when compared to the enzyme-bound aminoglycosides. These comparisons are shown in Figure 6, which clearly demonstrates that while the A and B rings are superimposable, the C rings can occupy a wide range of space.

These observations suggest that the conformational similarity of the bound aminoglycosides are not only valid for enzyme-aminoglycoside complexes but also include RNA-aminoglycoside complexes. It is clear that the aminoglycoside-modifying enzymes and RNA can provide appropriately positioned complementary groups to bind the aminoglycoside antibiotics in the same conformation using the same structural motif, which may have further implications for drug design to overcome the antibiotic resistance.

ACKNOWLEDGMENT

We thank Dr. Berghuis of the McGill University (Canada) for providing the preprint of his article that describes the X-ray structure of the aminoglycoside-3'-phosphotransferase with bound antibiotics.

REFERENCES

- Schatz, A., Bugie, E., and Walksman, S. A. (1944) *Proc. Soc. Exp. Biol. Med.* 55, 66–69.
- Davies, J. E. (1991) in *Antibiotics in Laboratory Medicine* (Lorian, V., Ed.) pp 691–713, Williams and Wilkins, Baltimore.
- Moazed, D., and Noller, H. F. (1987) *Nature* 327, 389–394.
- Umezawa, H. (1974) in *Advances in Carbohydrate Chemistry and Biochemistry* (Tipson, R. S., and Horton, D. Eds.) pp 183–225, Academic Press, New York.
- Davies, J. E. (1994) *Science* 264, 375–382.
- Shaw, K. J., Rather, P. N., Hare, R. S., and Miller, G. H. (1993) *Microbiol. Rev.* 57, 138–163.
- Cox, J. R., McKay, G. A., Wright, G. D., and Serpersu, E. H. (1996) *J. Am. Chem. Soc.* 118, 1295–1301.
- Cox, J. R., and Serpersu, E. H. (1997) *Biochemistry* 36, 2353–2359.
- Mohler, L. M., Cox, J. R., Serpersu, E. H. (1997) *Carbohydr. Lett.* 3, 17–24.
- DiGiammarino, E. L., Draker, K-a., Wright, G. D., and Serpersu, E. H. (1998) *Biochemistry* 37, 3638–3644.
- Cox, J. R., Ekman, D. R., DiGiammarino, E. L., Akal-Strader, A., Serpersu, E. H. (2000). *Cell Biochem. Biophys.* 33, 297–308.
- Serpersu, E. H., Cox, J. R., DiGiammarino, E. L., Mohler, M. L., Akal, A., Ekman, D. R., Owston, M. (2000). *Cell Biochem. Biophys.* 33, 309–321.
- Ekman, D. R., DiGiammarino, E. L., Wright, E., Witter, E. D., Serpersu, E. H. (2001). *Biochemistry* 40(24), 7017–7024.
- Sakon, J., Liao, H. H., Kanikula, A., M., Benning, M. M., Rayment, I., and Holden, H. M. (1993) *Biochemistry* 32, 11977–11984.
- Pedersen, L., C., Benning, M. M., and Holden, H. M. (1995) *Biochemistry* 34, 13305–13311.
- Hon, W.-C., McKay, G. A., Thompson, P. R., Sweet, R. M., Yang, D. S. C., Wright, G. D., and Berghuis, A. M. (1997) *Cell* 89, 887–895.
- Wybenga-Groot, L., Draker K-a., Wright, G., and Berghuis, A. M. (1999) *Structure* 7, 497–507.
- Wolf, E., Vassilev, A., Makino, Y., Sali, A., Nakatani, Y., and Burley, S. K. (1998) *Cell* 94, 439–449.
- Fong, D. H., and Berghuis, A. M. (2002) *EMBO J.* 21, 2323–2331.
- Fourmy, D., Recht, M. I., Blanchard, S. C., and Puglisi, J. D. (1996) *Science* 274, 1367–1371.
- Yoshizawa, S., Fourmy, D., and Puglisi, J. D. (1998) *EMBO J.* 17, 6437–6448.
- Jiang, L., Majumdar, A., Weidong, H., Jaishree, T. J., Weijun, X., and Patel, D. J. (1999) *Structure* 7, 817–827.
- Serpersu, E., H., and Owston, M. (2002) Abstract of the FASEB Meeting, New Orleans, April 20–24, 2002.
- Wright, G. D., and Ladak, P. (1997) *Antimicrob. Agents Chemother.* 41, 956–960.
- Williams, J. W. and Northrop, D. B. (1979). *J. Antibiot.* 32, 1147–1154.
- Vincent S. J. F., Zwahlen, C., and Bodenhausen, G. (1996) *J. Biomol. NMR* 7, 169–172.
- Zwahlen, C., Vincent, S. J. F., Di Bari, L., Levitt, M. H., and Bodenhausen, G. (1994). *J. Am. Chem. Soc.* 116, 362–368.
- Cox, J. R., and Serpersu, E. H. (1995) *Carbohydr. Res.* 271, 55–63.
- Homans, S. W. (1990). *Biochemistry* 29, 9110–9118.
- Vicens, Q., and Westhof, E. (2001) *Structure* 9, 647–658.

BI0261241